© 2014. Published by The Company of Biologists Ltd | The Journal of Experimental Biology (2014) 217, 1108-1115 doi:10.1242/jeb.092916

RESEARCH ARTICLE

Biomechanical strategies for mitigating collision damage in insect wings: structural design versus embedded elastic materials

Andrew M. Mountcastle* and Stacey A. Combes

ABSTRACT

The wings of many insects accumulate considerable wear and tear during their lifespan, and this irreversible structural damage can impose significant costs on insect flight performance and survivability. Wing wear in foraging bumblebees (and likely many other species) is caused by inadvertent, repeated collisions with vegetation during flight, suggesting the possibility that insect wings may display biomechanical adaptations to mitigate the damage associated with collisions. We used a novel experimental technique to artificially induce wing wear in bumblebees and yellowjacket wasps, closely related species with similar life histories but distinct wing morphologies. Wasps have a flexible resilin joint (the costal break) positioned distally along the leading edge of the wing, which allows the wing tip to crumple reversibly when it hits an obstacle, whereas bumblebees lack an analogous joint. Through experimental manipulation of its stiffness, we found that the costal break plays a critical role in mitigating collision damage in yellowjacket wings. However, bumblebee wings do not experience as much damage as would be expected based on their lack of a costal break, possibly due to differences in the spatial arrangement of supporting wing veins. Our results indicate that these two species utilize different wing design strategies for mitigating damage resulting from collisions. A simple inertial model of a flapping wing reveals the biomechanical constraints acting on the costal break, which may help explain its absence in bumblebee wings.

KEY WORDS: Hymenoptera, Insect, Resilin, Wear, Wing

INTRODUCTION

The wings of many insects experience cumulative and irreversible damage over the course of their lifespan (Alcock, 1996; Hayes and Wall, 1999; Cartar, 1992), and this can impose significant costs on insect flight performance and survivability. Wing area loss associated with wear and tear has been found to reduce vertical acceleration and predation success in dragonflies (Combes et al., 2010), alter foraging behavior in bees (Cartar, 1992; Foster and Cartar, 2011a; Haas and Cartar, 2008; Higginson and Barnard, 2004), and increase mortality in bumblebees (Cartar, 1992) and honeybees (Dukas and Dukas, 2011). Although the causal link between wing wear and increased mortality rates in bees has not been explicitly tested, it has been hypothesized that wing area loss reduces maneuverability and thus increases predation risk (Hedenstrom et al., 2001; Dukas and Dukas, 2011).

Wing damage in insects may result from a range of physical interactions, including those stemming from mating activity (Ragland and Sohal, 1973; Alcock, 1996), predation attacks (Shapiro, 1974) and collisions with vegetation (Wootton, 1992; Higginson and Gilbert, 2004; Foster and Cartar, 2011b). However, only one study has formally examined the cause of wing wear; Foster and Cartar (Foster and Cartar, 2011b) showed that wing area loss in foraging bumblebees was caused primarily by wing collisions with vegetation as the bees maneuvered in and around floral patches. They found that wings accidentally collided with vegetation relatively often – one strike per second on average – although these collisions occurred in bursts rather than at a constant rate (Foster and Cartar, 2011b). Our interpretation is that bees inadvertently move too close to plants while maneuvering through them or during takeoff and landing, causing their wings to repeatedly impact the vegetation at high frequencies until they move away or cease flapping. In this context, we expect the distal regions of the wing to experience the greatest frequency of collisions, and we expect abrasion to occur on both the ventral and dorsal sides of the wing (during both the downstroke and the upstroke). Foster and Cartar's results (Foster and Cartar, 2011b) suggest that many insects that forage on floral resources, as well as potentially all insects that fly in complex three-dimensional environments, may face similar wing collision risks and consequences. In light of the significant costs of wing wear to flight performance and survivability, insect wings may display biomechanical adaptations to mitigate the damage associated with collisions.

Insect wings are lightweight, flexible structures that consist primarily of hollow supporting veins and thin intervening membranes, with no intrinsic musculature (Wootton, 1992). Several recent studies show that wing flexibility is not merely an inherent liability of lightweight structures subjected to large external forces, but is in fact adaptive for a variety of functional demands, including aerodynamic force production and flight efficiency (Mountcastle and Combes, 2013; Young et al., 2009; Nakata and Liu, 2011). Wing flexibility in some insects is enhanced by mobile vein joints, which often contain embedded resilin, a rubber-like protein with low stiffness and high elastic efficiency (Weis-Fogh, 1961). Although relatively few studies have been conducted on the distribution and function of resilin joints in insect wings, these structures have been documented in beetle and earwig hind wings along fold lines that collapse the wing during rest (Haas et al., 2000b; Haas et al., 2000a), and in bumblebee and dragonfly wings along axes where the wings typically flex during flight (Gorb, 1999; Donoughe et al., 2011; Mountcastle and Combes, 2013). A recent study showed that a single resilin vein joint in the bumblebee wing (*Bombus impatiens*) contributes significantly to overall chordwise wing flexibility, and enhances vertical aerodynamic force capacity (Mountcastle and Combes, 2013).

The wings of many hymenopterans feature a flexible joint or 'costal break' along the leading edge of the wing, often located between the prestigma and stigma, and typically accompanied by a median flexion line that extends distally and posteriorly across the

Harvard University, Department of Organismic and Evolutionary Biology, Concord Field Station, 100 Old Causeway Road, Bedford, MA 01730, USA

*Author for correspondence (mountcastle@fas.harvard.edu)

Received 21 June 2013; Accepted 19 November 2013

The Journal of Experimental Biology

The Journal of Experimental Biology (2014) doi:10.1242/jeb.092916

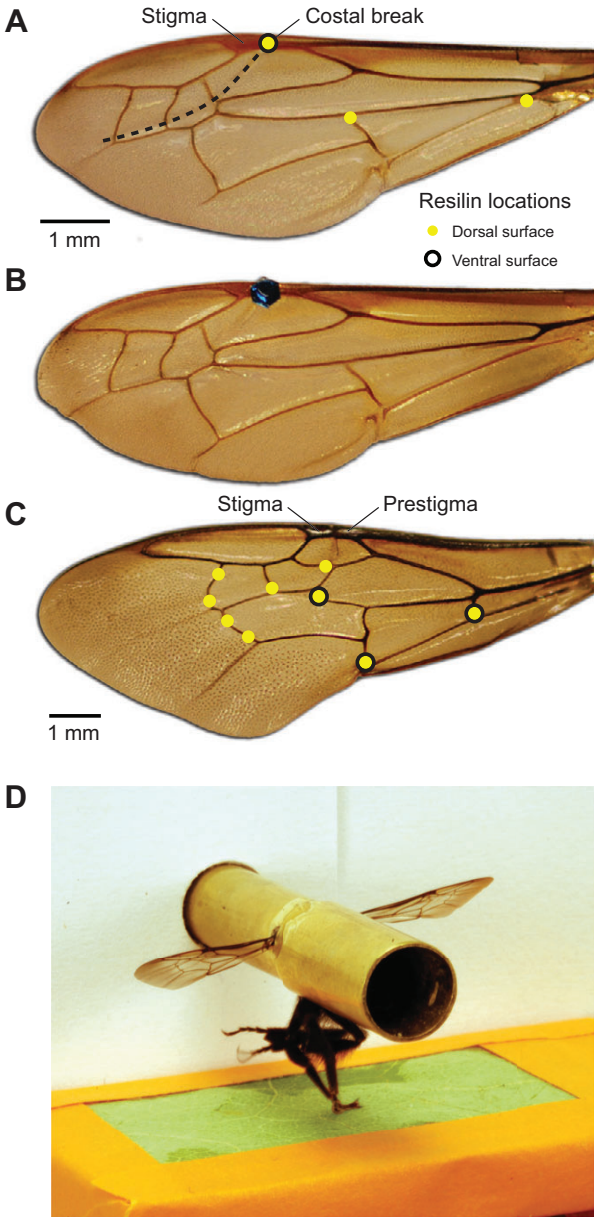

Fig. 1. Yellowjacket and bumblebee wing morphologies and experimental design. (A) Yellowjacket wing morphology: locations of embedded resilin in the yellowjacket forewing, mapped using fluorescence microscopy (340–380 nm excitation, 420 nm emission filter) (Donoughe et al., 2011). The dashed line indicates a median flexion line originating at the costal break between the prestigma and stigma. (B) Yellowjacket wing splint treatment: a piece of extra-fine polyester glitter (0.4 mm diameter, 20 µg) was affixed to the dorsal side of the yellowjacket wing, immobilizing the costal break (see supplementary material Movies 1, 2). (C) Bumblebee wing morphology: locations of embedded resilin in the bumblebee forewing, mapped in a previous study (Mountcastle and Combes, 2013). In contrast to the yellowjacket wing, the bumblebee wing does not have resilin or a flexible joint between the prestigma and stigma, and many of the major veins and vein junctions are located more proximally than in the yellowjacket. (D) Each bee or wasp was mounted in a custom-made brace designed to support the body and splay the wings apart, and positioned above a piece of leaf affixed with tape (orange perimeter) to an acrylic backing plate. The live insect was spun at 216 Hz for a total time of 60 min, forcing the left wing tip to repeatedly collide with the leaf surface at 75% wing span.

membrane (Wootton, 1981; Danforth and Michener, 1988; Michener, 2007). Using fluorescence microscopy, we mapped the distribution of resilin in the wing of the Eastern yellowjacket wasp (*Vespula maculifrons*), and found that the costal break contains embedded resilin on both its dorsal and ventral surfaces (Fig. 1A). Brackenbury (Brackenbury, 1994) used high-speed cinematography to examine hovering flight kinematics of representatives of several hymenopteran families, and found that the wing tips of some hymenoptera flexed at the costal break during ventral stroke reversal, coinciding with peak inertial force. Such wing tip deformations are thought to be aerodynamically beneficial, suggesting that the costal break and median flexion line in the wings of many hymenopterans may be adaptive for flight performance (Danforth, 1989; Wootton, 1981). We captured high-speed videography of yellowjackets flying in a flight chamber, and noticed that the costal break was regularly employed in a different sort of flight interaction: wings temporarily crumpled at the costal break whenever a wing tip collided with the walls or ceiling of the flight chamber.

Thus, we hypothesized that in addition to potentially conferring aerodynamic benefits, the costal break may also help to mitigate wing damage during collisions by allowing the wing tip to reversibly crumple when it hits an obstacle. Wootton identified a similar median flexion line in the wings of crane flies (order: Diptera), which he speculated might serve the same function (Wootton, 1992). Curiously, an analogous costal break and flexion line are absent from the wings of bumblebees (Fig. 1C), a genus that shares a common ancestor with wasps and displays similar life history traits. This circumstance presents an opportunity to both investigate the role of a flexible joint for mitigating collision damage and compare patterns of wing wear in two closely related insects with wings of similar size but distinct morphologies.

In this study, we used a novel experimental technique to artificially induce wing wear in Eastern yellowjacket wasps [*V. maculifrons* (Buysson 1905)] and common eastern bumblebees (*B. impatiens* Cresson 1863). To probe the role of the costal break in mitigating wing damage, we tested two groups of yellowjacket wings: one in which we immobilized the costal break with a micro-splint (Fig. 1B), and the other in which the wings remained unaltered (Fig. 1A). We tested only unaltered bumblebee wings, as these wings do not have a costal break to immobilize (Fig. 1C). To avoid the desiccation that occurs in isolated wings (Mengesha et al., 2011), we affixed live, intact insects to a custom-designed brace attached to a rotational motor and spun them at high frequencies, forcing the tip of the left forewing to repeatedly collide with the surface of a leaf (Fig. 1D; supplementary material Movies 1–3). We compared cumulative wing damage in splinted yellowjacket wings to (1) unaltered yellowjacket wings, to determine whether the costal break mitigates wing damage, and (2) bumblebee wings, to determine whether the lack of a costal break in this species results in levels of wing damage similar to those seen in splinted yellowjackets.

Finally, to gain insight into why costal breaks are present in the wings of some species and absent in others, we examined one potential liability of this feature – the possibility of the wing buckling at the costal break during normal flapping flight and disrupting aerodynamic force production. We created a quantitative model of a flapping wing with a flexible costal break, and asked under what circumstances a costal break would tend to buckle due to typical inertial flapping forces, becoming a liability to flight performance.

RESULTS

Wing wear

Splinted wasp wings lost more area than both unsplinted wasp wings and bumblebee wings, and accumulated damage at a much faster rate

The Journal of Experimental Biology (2014) doi:10.1242/jeb.092916

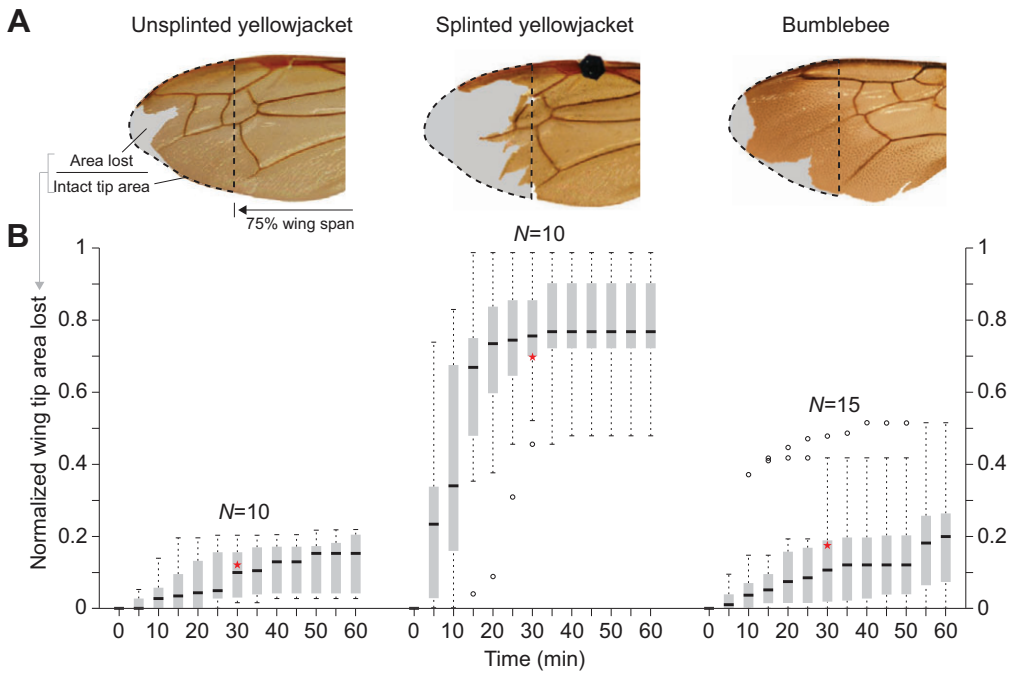

Fig. 2. Results of wing wear experiments. (A) Sample photographs of wings in each treatment group after 30 min (388,800 collisions). (B) Cumulative loss of wing tip area for wings in each treatment group over 60 min, measured every 5 min (77,760 collisions). The amount of tip area lost at each time step was normalized by the total intact tip area. Red stars indicate the data points corresponding to the photographs shown in A.

than the other two groups (Fig. 2). There was a statistically significant difference between the groups at every time interval, as determined by a one-way ANOVA ($F_{2,32}$≥10.478, P<0.0001 at every interval). A Fisher's least significance difference test revealed that wing area loss in the splinted yellowjacket group was significantly higher than in both the unsplinted yellowjacket group (P<0.0001 at every interval) and the bumblebee group (P<0.0001), which were never significantly different from each other (P≥0.221 at every interval).

After only 5 min (64,800 collisions), the splinted yellowjacket wings had not only lost more area on average (normalized area lost 0.23±0.23) than either the unsplinted yellowjacket wings (0.01±0.02) or the bumblebee wings (0.02±0.03) but also already exceeded the total area lost by either of these groups over the entire duration of the trial (777,600 collisions) in only 1/12th of the time (Fig. 2B). After 15 min (194,400 collisions), the mean normalized area loss in splinted yellowjacket wings was 0.61±0.27, compared with 0.06±0.06 for unsplinted yellowjacket wings and 0.10±0.14 for bumblebee wings. While the splinted yellowjacket wings experienced a much higher rate of wing wear initially, their rate of area loss started to diminish after 15 min, and area loss eventually plateaued at 0.77±0.16 by 35 min (453,600 collisions). In contrast, the unsplinted yellowjacket wings and bumblebee wings continued to gradually lose wing area over time, ultimately reaching 0.13±0.08 and 0.20±0.15, respectively, by the end of the 60 min trial. Thus, relative to the splinted yellowjacket wings, unaltered yellowjacket wings had lost only 6% as much area after 5 min of collisions, and this relative area loss rose slowly to 9%, 13% and 17% after 15, 30 and 60 min, respectively. Similarly, bumblebee wings had lost only 10% as much area as splinted yellowjacket wings after 5 min, rising to 16%, 18% and 26% relative area loss after 15, 30 and 60 min.

Inertial model

Our quantitative model reveals that in order to maintain wing integrity (i.e. avoid buckling) during flapping flight, the costal break in yellowjacket wings must withstand a maximum moment of 0.276 mN mm at stroke reversal, while the bumblebee prestigma–stigma junction must withstand 1.933 mN mm, a moment that is ~7 times greater.

DISCUSSION

Wing wear

In this study, we subjected each wing to a total of 777,600 collisions over 60 min, which we estimate to be within the range of the total number of wing collisions that bumblebee foragers are likely to experience over the course of their lifespan. Based on a wing collision frequency of 1 strike s^{-1} (Foster and Cartar, 2011b), an average daily foraging time of 7.5 h (Crall and Combes, 2013) and a life expectancy ranging from 13 days (Rodd et al., 1980) to 34 days (Goldblatt and Fell, 1987), a bumblebee would amass 351,000 to 918,000 wing collisions over its lifespan – a range that encompasses the 777,600 collisions we applied. Yellowjackets may not spend as much time each day maneuvering through plants, as they are omnivores who obtain their protein by hunting and scavenging other insects, rather than by gathering pollen. Nevertheless, they do spend a considerable amount of time foraging for floral nectar (their primary energy source) (Parrish and Fowler, 1983), as well as maneuvering through other complex three-dimensional habitats while hunting; thus, their wing collision rates are likely to be similar.

Splinting the costal break in yellowjacket wings caused a dramatic acceleration in the rate of wing wear compared with unsplinted wings, demonstrating that the costal break plays a critical role in mitigating collision damage in wasp wings. After losing over 60% of their wing tip area in only 15 min, however, the rate of area loss in splinted yellowjacket wings started to decline, and no further area loss occurred once the tip had worn down to 23% of its original area after 35 min. This asymptotic wing area loss over time can be explained by the combination of two factors: reduced structural support with increasing wing wear, and a reduction in the wing–leaf contact zone with decreasing wing span (Fig. 3). As the wing tip becomes progressively frayed and tattered, the sections of wing that remain form isolated projections, with less structural reinforcement from the surrounding wing area (e.g. see the splinted yellowjacket wing tip in Fig. 2A). These unreinforced (and thus more flexible) projections tend to bend out of the way more easily during collisions, diminishing the rate of further wing wear.

The Journal of Experimental Biology (2014) doi:10.1242/jeb.092916

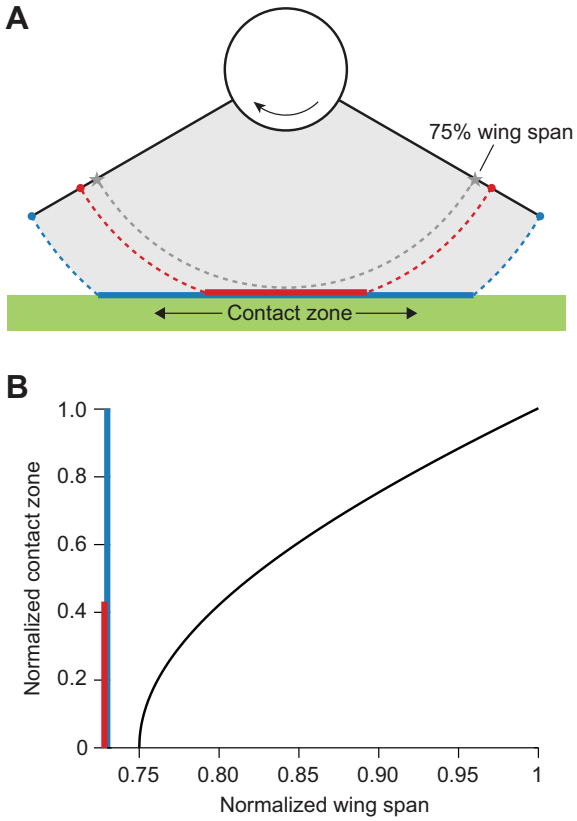

Fig. 3. Wing–leaf contact zone is dependent on distance along the wing span. (A) Schematic diagram illustrating the trajectory of a rotating wing as it collides with a surface (green wall) aligned at 75% of wing span (gray star). The tip of the wing (blue dot) sweeps the largest circular arc (dashed blue line) and therefore has the longest contact zone (solid blue line) with the surface obstacle. More proximal regions of the wing (red) have shorter contact zones. (B) Wing–leaf contact zone decreases non-linearly, moving in from the wing tip to the point where the wing just contacts the obstacle (75% of span in this study), according to Eqn 1. This relationship helps explain why wing area loss in the splinted yellowjacket wings approaches an asymptote as the tip of the wing is progressively lost (Fig. 2).

In addition, the distance across which a wing section is dragged during a collision (the 'contact zone') depends on the spanwise position, with the outer-most region of the wing tip experiencing the longest contact zone and the inner-most region of the wing tip (approaching 75% wing span) experiencing the shortest contact zone (Fig. 3A). A basic geometric analysis reveals that this relationship between spanwise position and contact zone is non-linear; contact zone diminishes at an increasing rate with decreasing spanwise position (Fig. 3B):

$$\mathrm{cz} = 2p\sqrt{1 - c^2 s^2 / p^2}\,, \qquad (1)$$

where cz is the contact zone, p is the spanwise position, c is the normalized position of the obstacle relative to the intact wing span (0.75 in this study) and s is the intact wing span. The implication of this relationship is that the proximal region of the wing tip has a relatively small contact zone over which physical interaction with the leaf surface can cause damage, and this region therefore experiences a much slower rate of wear compared with the distal wing tip. This span-dependent wear phenomenon may be less relevant in natural contexts, where obstacles are not likely to be encountered at a fixed location, as in our assay; however, the reduced wear due to decreased structural support in tattered wings would still occur. Thus, future studies quantifying ongoing wing damage in bees foraging in natural settings would provide valuable information about the temporal progression of wing damage in wild insects.

The amount of wing damage accrued by splinted yellowjacket wings in this study would have considerable consequences in a natural context, underscoring the adaptive significance of a flexible joint for mitigating wing wear in wasps. Cartar found that an 18% reduction in wing surface area from the outer margin of each forewing caused a significant reduction in bumblebee life expectancy in the field (Cartar, 1992). The wing tip region that we focused on during this study makes up ~27% of the entire wing surface in both yellowjackets and bumblebees; thus, losing 67% of this tip area is equivalent to an 18% reduction in total wing area. The majority of yellowjacket wings with a splinted costal break accumulated this amount of wing wear [enough to likely affect their mortality rate based on Cartar's results for bumblebees (Cartar, 1992)] after only 15 min, or 194,400 collisions. In contrast, neither the unsplinted yellowjacket wings nor the bumblebee wings lost 18% of their total wing surface area over the entire trial (Fig. 2B). Our results show that while the costal break is essential for mitigating collision damage in yellowjacket wings, bumblebee wings do not experience the accelerated wear that might be expected, based on their lack of a costal break. Why do wasp wings need a costal break to mitigate wing wear, while bumblebee wings do not?

A comparison of yellowjacket and bumblebee wing morphologies suggests that these two species rely on alternative biomechanical strategies for mitigating wing damage due to collisions. Wing veins provide the structural support for insect wings (Wootton, 1992), and hymenopteran wings typically possess a similar complement of major veins and vein junctions (Fig. 1). Despite possessing many of the same veins and vein junctions, however, the distribution of these structures within the wing can vary substantially between species. In yellowjackets, the veins extend all the way to the wing tip, supporting the distal-most region of the wing (Fig. 1A). In contrast, bumblebee wing veins are withdrawn to more proximal regions of the wing and do not extend much beyond 75% of the wing span (Fig. 1C), leaving the entire distal region unreinforced and more continuously flexible than the veined yellowjacket wing tip. Thus, whereas a costal break is necessary in yellowjackets to allow an otherwise rigid wing to buckle upon contact with an obstacle (Fig. 4A,B; supplementary material Movies 1, 2), we presume that it is less important in bumblebees, as their vein-less wing tip is inherently more flexible overall (Fig. 4C; supplementary material Movie 3). However, just because a costal break is less important for mitigating wing wear in bumblebees, this is not a sufficient explanation for its absence in the bumblebee wing, when other hymenoptera representatives display both withdrawn wing veins and a costal break (Danforth, 1989; Danforth and Michener, 1988). The absence of a costal break in bumblebees may have nothing to do with wing wear per se, but might instead relate to biomechanical constraints on the costal break associated with flapping flight.

Inertial model

Representatives of some hymenopteran families display ventral wing flexion at the costal break during hovering flight, while members of other families, including the vespid wasps, display little or no deformation of the wing tip (Brackenbury, 1994). Consistent

The Journal of Experimental Biology (2014) doi:10.1242/jeb.092916

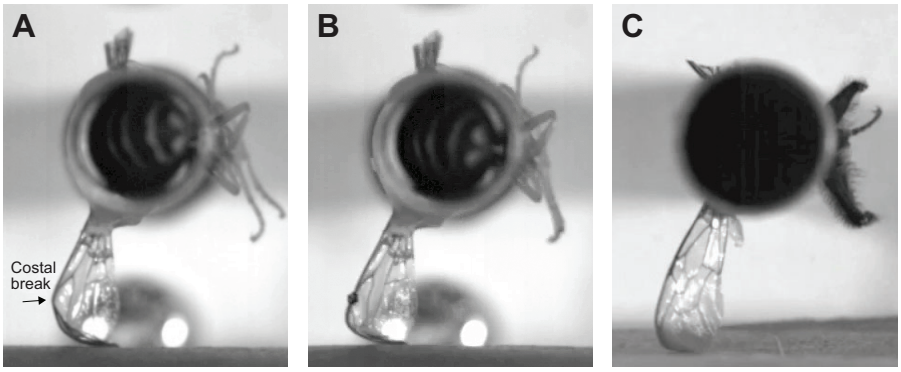

Fig. 4. Still frame images of each wing treatment at mid-collision. (A) Unsplinted yellowjacket wing. The wing naturally flexes at the costal break when the wing tip collides with the leaf surface. (B) Splinted yellowjacket wing. The glitter splint immobilizes the costal break, forcing the relatively stiff wing tip to bend sharply and greatly accelerating wing wear. (C) Bumblebee wing. As a result of reduced venation, the bumblebee wing tip is more continuously flexible than the yellowjacket wing tip, resulting in a more gradual bend distributed across the tip region. Thus, bumblebee wings do not experience as much wear as would be expected based on their lack of a costal break.

with prior observations, we did not see any flexion at the costal break in our high-speed video analysis of yellowjackets during hovering flight (except during wing collisions). Therefore, the costal break must be either stiff enough to prevent wing tip flexion entirely during flight (in the case of vespids, for example) or to allow moderate tip deflection but prevent complete wing buckling, which would likely disrupt aerodynamic force production.

Most hymenopterans display a consistent pattern of size-related changes in wing venation that is thought to be related to the forces their wings experience during flight. Danforth (Danforth, 1989) found that with increasing body size, the distal-most wing cells tend to become elongated and the veins extend further towards the tip, and with decreasing body size the opposite occurs. Danforth hypothesized that the distal extension of wing veins in larger hymenoptera helps their larger wings withstand increased bending moments, whereas the withdrawal of wing venation in smaller hymenoptera reduces the wing's moment of inertia, allowing for the relatively higher wingbeat frequencies needed to overcome the high coefficients of skin friction drag in small insects (Danforth, 1989). Although the costal break was not the focus of Danforth's study, he did not report any size-related trends in the presence or absence of a costal break, and indeed at least three families (Sphecidae, Anthophoridae and Andrenidae) appear to feature both small and large representatives that display a costal break (Danforth, 1989). The size-related wing venation trend described by Danforth would appear to explain the venation differences we observed between bumblebees and yellowjackets, except for the fact that the allometric scaling is reversed: bumblebees are larger (162±21 mg, N=15) but display withdrawn veins, while yellowjackets are smaller (61±19 mg, N=20) but display elongated veins. Yellowjackets in fact follow the trend seen in most hymenoptera, whereas bumblebees appear to be an outlier; in addition to having unusually withdrawn wing veins for their size, they also have an unusually high wingbeat frequency (Greenewalt, 1962). Our inertial model shows that this combination of extreme wing morphology and kinematics (for their size) substantially increases the moments experienced by the wings during flight, and thus may help explain why bumblebees do not have a costal break, in contrast to many other hymenopterans, both larger and smaller.

As our model shows (see Eqn 2 in Materials and methods; Fig. 5), the maximum inertial moment at the costal break increases linearly with stroke amplitude, and non-linearly with flapping frequency, wing span and spanwise joint position. In particular, the applied moment has a cubic relationship with wing span and joint position, and is therefore extremely sensitive to any morphological differences in these parameters. This equation supports Danforth's hypothesis that size-related changes in wing venation may help compensate for changes in inertial loading with size (Danforth, 1989): as wing span increases, the tendency towards increased applied moment at the costal break is partially offset by the distal extension of wing venation (including the costal break itself), which reduces the moment of inertia of the wing tip segment. As already mentioned, however, bumblebee wings do not follow this trend.

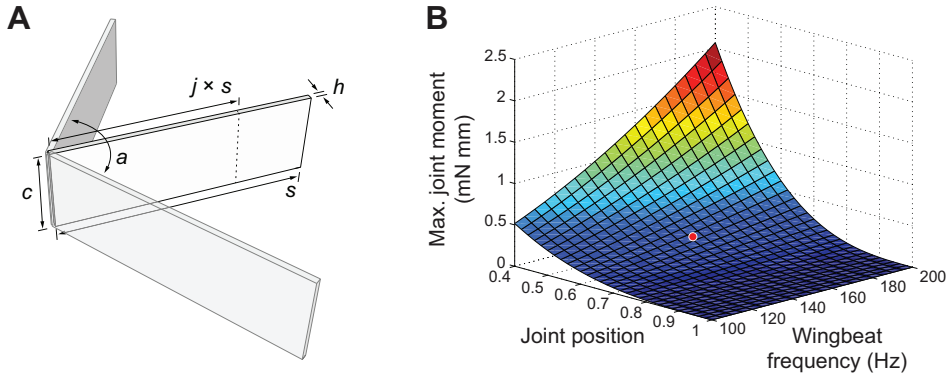

Fig. 5. Inertial model of a simplified, flapping insect wing with a flexible costal break. (A) We modeled a wing as a rectangular plate (with span s, chord length c and thickness h) subject to sinusoidal flapping kinematics (of amplitude a and frequency f), and calculated the maximum inertial moment at stroke reversal about a costal break (represented by the dashed line, at normalized spanwise position j), according to Eqn 2. (B) Model results for a wing with the dimensions (s=9.07 mm, c=2.02 mm, h=10 μm) and stroke amplitude (a=115 deg) of a yellowjacket. Joint moment increases non-linearly as wing beat frequency rises ($\mathbf{M}\propto f^2$) and as the flexible joint moves closer to the wing base [$\mathbf{M}\propto(1-j)^3$; see Eqn 2]. The red dot marks the maximum joint moment calculated for a yellowjacket wing (0.276 mN mm), based on a joint position of 0.63 and a wingbeat frequency of 151 Hz. Bumblebee wings experience a maximum joint moment (based on their wing morphology and kinematics) that is approximately seven times greater than this (1.933 mN mm).

The Journal of Experimental Biology (2014) doi:10.1242/jeb.092916

Although bumblebee wings are nearly equal in length to yellowjacket wings, their substantially greater wing tip moment of inertia and much higher wingbeat frequency mean that if they were to have a flexible joint between the prestigma and stigma, it would need to be stiff enough to withstand periodic force moments that are roughly 700% greater than those experienced by a yellowjacket costal break, in order to prevent the wing tip from buckling during flight. Although it is not self-evident whether a sevenfold increase in applied moment necessarily imposes a biomechanical constraint on a wing joint (as a wing's capacity to resist moments depends on its second moment of area, which scales by a linear dimension to the fourth power), this is nevertheless a rather large difference for wings of similar size.

Biomechanical constraints on joint stiffness during flapping flight might therefore help explain why bumblebees, as well as other hymenopterans that experience particularly large inertial loads, lack a costal break. At least one other representative appears to support this hypothesis: honeybees also have an unusually high wingbeat frequency relative to their wing span (Greenewalt, 1962; Altshuler et al., 2005), and their wings also lack a costal break. In general, a phylogeny mapping the gain and loss of the costal break in hymenoptera would greatly improve our understanding of the factors and constraints acting on this morphological feature, and ongoing work is aimed at this goal.

SUMMARY

Although the results of this study clearly demonstrate the utility of a costal break for mitigating wing collision damage, the extent to which wing wear exerts a selective pressure that has contributed to the evolution, maintenance or loss of the costal break remains unknown. As mentioned above, the wings of several hymenopterans display ventral flexion at the costal break during stroke reversal while hovering, which is thought to serve an aerodynamic function (although this has not been explicitly tested). Other hymenoptera, including the vespids, do not display flexion at the costal break during hovering flight (Brackenbury, 1994), but could display joint flexion during more challenging flight maneuvers or when carrying heavy loads (Nachtigall, 2000). Thus, it is possible that aerodynamic function is the primary selective pressure responsible for the evolution and maintenance of a costal break in hymenoptera, and mitigation of wing wear is merely a secondary benefit. It is also possible that the costal break may have originally evolved for an aerodynamic function, but has since experienced a functional shift in some groups, such that its benefits in terms of mitigating wing wear are now primarily responsible for its continued presence.

It should be noted that the artificial wing wear experiments in this study do not account for the full complexity and variability of collisions that wings may experience in nature, which likely occur at all phases of the stroke cycle (including during the upstroke and downstroke), over a range of impact speeds, and in many different orientations, and which involve plant structures that often have some degree of flexibility themselves. Furthermore, the extent to which wing wear is affected by natural variability in the surface roughness of vegetation (Whitney and Federle, 2013) is completely unknown, but this is an area that deserves further exploration.

Wing wear is a widespread phenomenon among many flying insects, and it occurs consistently enough that it serves as a reliable indicator of age in some insects (Mueller and Wolf-Mueller, 1993). Yet, recent studies have shown that wing wear has serious behavioral and functional consequences, suggesting that insect wings may display adaptations that allow them to minimize such damage. Here we show that two closely related species of hymenopterans rely on different biomechanical strategies for mitigating the wing wear that results from collisions with vegetation during flapping flight. This study thus sheds light on a potential evolutionary pressure acting on insect wing design that has been previously overlooked, and adds to our growing understanding of the functional significance of insect wing diversity.

MATERIALS AND METHODS

Subjects

Yellowjacket wasps (*V. maculifrons*) were collected during summer and autumn of 2012 at floral patches around the Concord Field Station in Bedford, MA, USA, and at a nearby ice cream stand. Wasps were stored in a small flight cage in the laboratory that contained cotton balls soaked in a 50% sugar solution, and all experiments were performed within 48 h of capture. Bumblebee hives (*B. impatiens*) were purchased from International Technology Services and stored in a 0.6×0.6×1.8 m netting enclosure in the laboratory. The bees had access to a reservoir of artificial nectar (50% sugar solution) within the hive, and could enter and leave the hive freely to explore the surrounding enclosure.

Wing wear assay

We tested wing wear in three treatment groups: unsplinted yellowjacket wings, splinted yellowjacket wings and bumblebee wings. To splint the costal break in yellowjacket wings, we glued a single piece of extra-fine polyester glitter across the joint with cyanoacrylate adhesive, following a previously described method (Mountcastle and Combes, 2013). Each insect was cold anesthetized at −15°C for ~5 min until the first signs of quiescence, then promptly removed from the freezer and mounted in a custom-designed brace attached to the shaft of a brushed DC motor (Pololu 25D × 48L, Fig. 1D). The brace was designed to support the insect body and splay its wings apart. We measured wing wear on the left forewing, first removing the right wing pair and left hindwing, then measuring span length of the left forewing with digital calipers and adding a drop of cyanoacrylate adhesive to the base of the forewing to fix its position relative to the brace. For wasps in the splinted treatment, we then attached a piece of glitter across the costal break (see Mountcastle and Combes, 2013).

The insect was positioned above a piece of Japanese knotweed leaf affixed to an acrylic backing plate (Fig. 1D). Japanese knotweed (*Fallopia japonica*) is a large-leafed, herbaceous, perennial plant that attracts both bumblebee and yellowjacket foragers during its late summer bloom in New England, and we observed the wings of these insects periodically colliding with leaves during foraging activity. Prior to each trial, we cut a fresh 3×6 cm section from a Japanese knotweed leaf and affixed it to the backing plate with lab tape. We positioned the leaf surface such that the ventral side of the rotating left wing tip would collide with it at 75% wing span (Fig. 2A).

We spun each bee and wasp in continuous rotation at 216 Hz (subjecting it to 216 wing collisions per second) for a total time of 60 min (supplementary material Movies 1–3). The wings rotated at an angular velocity of 77,760 deg s^{-1}, which is ~95% of the maximum angular velocity a bumblebee wing experiences during flapping flight [based on a sinusoidal wingbeat frequency of 181 Hz and a horizontally projected stroke amplitude of 144 deg. (Buchwald and Dudley, 2010)], and 143% of the maximum angular velocity a yellowjacket wing experiences (based on a sinusoidal wingbeat frequency of 151 Hz and a horizontally projected stroke amplitude of 115 deg, as measured below). We stopped the motor every 5 min to photograph the left forewing from the dorsal aspect.

We analyzed photographs to measure the wing tip area lost at each time interval as a result of repeated collisions with the leaf. Each image was cropped to include only the distal 25% of the wing (outlines in Fig. 2A), and we used the quick selection tool in Adobe Photoshop CS6 (v13.0.4, Adobe Systems Inc., San Jose, CA, USA) to select and measure the wing tip surface area remaining. We calculated the normalized wing tip area lost as the difference between the original intact area of the pristine wing tip and the remaining surface area, divided by the intact tip area (Fig. 2A).

Inertial model

Prior work has shown that inertial loads largely dominate in determining patterns of passive wing bending at this scale (Combes and Daniel, 2003b; Daniel and Combes, 2002; Ramananarivo et al., 2011), and the maximum inertial moment typically occurs at stroke reversal, when acceleration is greatest. Thus, we created a simplified model of an insect wing, treating the wing as a uniform rectangular plate undergoing a sinusoidal flapping motion along a single axis of rotation, and calculated the maximum moment of inertial force applied about a chordwise axis representing the costal break and median flexion line (Fig. 5A, dotted line). The maximum magnitude of the inertial moment applied to the costal break at stroke reversal can be approximated as:

$$M = I\alpha = \frac{1}{270} a\, c f^2\, h\, \rho\, \pi^3\, s^3 (1-j)^3\,, \qquad (2)$$

where I is moment of inertia of the wing section distal to the costal break, α is angular acceleration, a is wing stroke amplitude (deg), f is wingbeat frequency (Hz), j is normalized position of the costal joint along the wing span, s is total wing span, c is wing chord, h is wing thickness and ρ is wing density (Fig. 5A).

Using this model, we estimated the maximum moment of force applied about the costal break in yellowjacket wings, and about the prestigma–stigma junction in bumblebee wings, based on their respective wing morphologies and kinematics. We analyzed the initial photographs of all experimental wings in Adobe Photoshop CS6 to measure their morphological parameters. Yellowjacket wings (N=20) had a mean wing span of 9.07±0.84 mm, a chord length of 2.89±0.24 mm and a normalized costal break position of 0.63±0.01. Bumblebee wings (N=15) had a mean span of 9.87±0.59 mm, a chord length of 3.33±0.36 mm and a normalized prestigma–stigma junction position of 0.49±0.02 (substantially closer to the wing base than in yellowjackets). We defined chord length (c) of our model wings as 70% of the measured maximum chord length of real wings, to partially account for the natural contraction of chord length with wing span. We chose a thickness (h) of 10 μm for both of our model wings (Tanaka et al., 2011), and a material density (ρ) of 1200 kg m^{-3} (Combes and Daniel, 2003a).

To determine wingbeat frequency (f) and stroke amplitude (a), we captured high-speed videos of yellowjackets by placing them in a flight chamber and filming from above at 1000 frames s^{-1}. We quantified stroke amplitude by digitizing two points along the leading edge of each forewing (one near the wing base and the other at mid-wing) at 10 consecutive stroke reversals using MATLAB digitization software (Hedrick, 2008), and calculated the mean swept angle of both wings across five strokes. We calculated mean wingbeat frequency over 20–40 complete strokes in each individual. We found a mean stroke amplitude of 115±7 deg and wingbeat frequency of 151±9 Hz (N=5) for yellowjackets, and used previously published measurements of wingbeat frequency (181 Hz) and stroke amplitude (144 deg) for *B. impatiens* bumblebees (Buchwald and Dudley, 2010). These kinematic parameters, together with the morphological measurements above, were used in Eqn 2 to estimate inertial force moments about the costal break in yellowjackets and the prestigma/stigma junction in bumblebees.

Acknowledgements

We thank Ifedayo Kuye for his assistance mapping resilin structures in the bumblebee and yellowjacket wing, Ivo Ros and Allison Arnold for their helpful comments on this manuscript, and Kimball Farm for providing delicious nectar to both yellowjackets and researchers alike.

Competing interests

The authors declare no competing financial interests.

Author contributions

A.M.M. and S.A.C. conceived the study. A.M.M. designed and executed the experiments. A.M.M. and S.A.C. interpreted the findings, and drafted and revised the article.

Funding

This work was supported by a National Science Foundation Expeditions in Computing Grant [grant number CCF-0926148].

Supplementary material

Supplementary material available online at
http://jeb.biologists.org/lookup/suppl/doi:10.1242/jeb.092916/-/DC1

References

Alcock, J. (1996). Male size and survival: the effects of male combat and bird predation in Dawson's burrowing bees, *Amegilla dawsoni*. *Ecol. Entomol.* **21**, 309-316.
Altshuler, D. L., Dickson, W. B., Vance, J. T., Roberts, S. P. and Dickinson, M. H. (2005). Short-amplitude high-frequency wing strokes determine the aerodynamics of honeybee flight. *Proc. Natl. Acad. Sci. USA* **102**, 18213-18218.
Brackenbury, J. H. (1994). Hymenopteran wing kinematics: a qualitative study. *J. Zool. (Lond.)* **233**, 523-540.
Buchwald, R. and Dudley, R. (2010). Limits to vertical force and power production in bumblebees (Hymenoptera: *Bombus impatiens*). *J. Exp. Biol.* **213**, 426-432.
Cartar, R. V. (1992). Morphological senescence and longevity: an experiment relating wing wear and life span in foraging wild bumble bees. *J. Anim. Ecol.* **61**, 225-231.
Combes, S. A. and Daniel, T. L. (2003a). Flexural stiffness in insect wings. II. Spatial distribution and dynamic wing bending. *J. Exp. Biol.* **206**, 2989-2997.
Combes, S. A. and Daniel, T. L. (2003b). Into thin air: Contributions of aerodynamic and inertial-elastic forces to wing bending in the hawkmoth *Manduca sexta*. *J. Exp. Biol.* **206**, 2999-3006.
Combes, S. A., Crall, J. D. and Mukherjee, S. (2010). Dynamics of animal movement in an ecological context: dragonfly wing damage reduces flight performance and predation success. *Biol. Lett.* **6**, 426-429.
Crall, J. D. and Combes, S. A. (2013). Blown in the wind: Bumblebee temporal foraging patterns in naturally varying wind conditions. *Integr. Comp. Biol.* **53**, E270.
Danforth, B. N. (1989). The evolution of hymenopteran wings: the importance of size. *J. Zool. (Lond.)* **218**, 247-276.
Danforth, B. N. and Michener, C. D. (1988). Wing folding in the Hymenoptera. *Ann. Entomol. Soc. Am.* **81**, 342-349.
Daniel, T. L. and Combes, S. A. (2002). Flexible wings and fins: bending by inertial or fluid-dynamic forces? *Integr. Comp. Biol.* **42**, 1044-1049.
Donoughe, S., Crall, J. D., Merz, R. A. and Combes, S. A. (2011). Resilin in dragonfly and damselfly wings and its implications for wing flexibility. *J. Morphol.* **272**, 1409-1421.
Dukas, R. and Dukas, L. (2011). Coping with nonrepairable body damage: effects of wing damage on foraging performance in bees. *Anim. Behav.* **81**, 635-638.
Foster, D. J. and Cartar, R. V. (2011a). Wing wear affects wing use and choice of floral density in foraging bumble bees. *Behav. Ecol.* **22**, 52-59.
Foster, D. J. and Cartar, R. V. (2011b). What causes wing wear in foraging bumble bees? *J. Exp. Biol.* **214**, 1896-1901.
Goldblatt, J. W. and Fell, R. D. (1987). Adult longevity of workers of the bumble bees *Bombus fervidus* (F.) and *Bombus pennsylvanicus* (De Geer) (Hymenoptera: Apidae). *Can. J. Zool.* **65**, 2349-2353.
Gorb, S. N. (1999). Serial elastic elements in the damselfly wing: mobile vein joints contain resilin. *Naturwissenschaften* **86**, 552-555.
Greenewalt, C. H. (1962). Dimensional relationships for flying animals. *Smithsonian Misc Collections* **144**, 1-46.
Haas, C. A. and Cartar, R. V. (2008). Robust flight performance of bumble bees with artificially induced wing wear. *Can. J. Zool.* **86**, 668-675.
Haas, F., Gorb, S. and Wootton, R. J. (2000a). Elastic joints in dermapteran hind wings: materials and wing folding. *Arthropod Struct. Dev.* **29**, 137-146.
Haas, F., Gorb, S. and Blickhan, R. (2000b). The function of resilin in beetle wings. *Proc. Biol. Sci.* **267**, 1375-1381.
Hayes, E. J. and Wall, R. (1999). Age-grading adult insects: a review of techniques. *Physiol. Entomol.* **24**, 1-10.
Hedenstrom, A., Ellington, C. P. and Wolf, T. J. (2001). Wing wear, aerodynamics and flight energetics in bumblebees (*Bombus terrestris*): an experimental study. *Funct. Ecol.* **15**, 417-422.
Hedrick, T. L. (2008). Software techniques for two- and three-dimensional kinematic measurements of biological and biomimetic systems. *Bioinspir. Biomim.* **3**, 034001.
Higginson, A. D. and Barnard, C. J. (2004). Accumulating wing damage affects foraging decisions in honeybees (*Apis mellifera* L.). *Ecol. Entomol.* **29**, 52-59.
Higginson, A. D. and Gilbert, F. (2004). Paying for nectar with wingbeats: a new model of honeybee foraging. *Proc. Biol. Sci.* **271**, 2595-2603.
Mengesha, T. E., Vallance, R. R. and Mittal, R. (2011). Stiffness of desiccating insect wings. *Bioinspir. Biomim.* **6**, 014001.
Michener, C. D. (2007). *The Bees of the World*. Baltimore, MD: The Johns Hopkins University Press.
Mountcastle, A. M. and Combes, S. A. (2013). Wing flexibility enhances load-lifting capacity in bumblebees. *Proc. Biol. Sci.* **280**, 20130531.
Mueller, U. and Wolf-Mueller, B. (1993). A method for estimating the age of bees: Age-dependent wing wear and coloration in the Wool-Carder bee Anthidium manicatum (hymenoptera: Megachilidae). *J. Insect Behav.* **6**, 529-537.
Nachtigall, W. (2000). Insect wing bending and folding during flight without and with an additional prey load. *Entomologia Generalis* **25**, 1-16.
Nakata, T. and Liu, H. (2011). Aerodynamic performance of a hovering hawkmoth with flexible wings: a computational approach. *Proc. Biol. Sci.* **279**, 722-731.
Parrish, M. D. and Fowler, H. G. (1983). Contrasting foraging related behaviours in two sympatric wasps (*Vespula maculifrons* and *V. germanica*). *Ecol. Entomol.* **8**, 185-190.
Ragland, S. S. and Sohal, R. S. (1973). Mating behavior, physical activity and aging in the housefly, *Musca domestica*. *Exp. Gerontol.* **8**, 135-145.

Ramananarivo, S., Godoy-Diana, R. and Thiria, B. (2011). Rather than resonance, flapping wing flyers may play on aerodynamics to improve performance. *Proc. Natl. Acad. Sci. USA* **108**, 5964-5969.
Rodd, F. H., Plowright, R. C. and Owen, R. E. (1980). Mortality rates of adult bumble bee workers (Hymenoptera: Apidae). *Can. J. Zool.* **58**, 1718-1721.
Shapiro, A. M. (1974). Beak-mark frequency as an index of seasonal predation intensity on common butterflies. *Am. Nat.* **108**, 229-232.
Tanaka, H., Whitney, J. P. and Wood, R. J. (2011). Effect of flexural and torsional wing flexibility on lift generation in hoverfly flight. *Integr. Comp. Biol.* **51**, 142-150.
Weis-Fogh, T. (1961). Molecular interpretation of the elasticity of resilin, a rubber-like protein. *J. Mol. Biol.* **3**, 648-667.
Whitney, H. M. and Federle, W. (2013). Biomechanics of plant-insect interactions. *Curr. Opin. Plant Biol.* **16**, 105-111.
Wootton, R. J. (1981). Support and deformability in insect wings. *J. Zool.* **193**, 447-468.
Wootton, R. J. (1992). Functional morphology of insect wings. *Annu. Rev. Entomol.* **37**, 113-140.
Young, J., Walker, S. M., Bomphrey, R. J., Taylor, G. K. and Thomas, A. L. R. (2009). Details of insect wing design and deformation enhance aerodynamic function and flight efficiency. *Science* **325**, 1549-1552.